Inorg. Chem. **1996,** *35,* 7924−7927

Microwave Irradiation Synthesis of Mo(W)/Tl/S Linear Chains and Their Nonlinear Optical Properties in Solution

Jianping Lang,[†] Kazuyuki Tatsumi,[*,†]
Hiroyuki Kawaguchi,[†] Jianmei Lu,[‡] P. Ge,[§]
W. Ji,[§] and Shu Shi[§]

Department of Chemistry, Faculty of Science,
Nagoya University, Furo-cho, Chikusa-ku,
Nagoya 464, Japan, Department of Chemistry,
Suzhou University, Suzhou 215006, P. R. China,
and Optical Crystal Laboratory, Department of Chemical
Engineering, and Department of Physics,
National University of Singapore, Singapore 0511, Singapore

Received September 6, 1996

Introduction

In recent years, several elegant techniques for solid state synthesis at mild reaction conditions have been developed for the preparation of new materials having interesting electronic, optical, and catalytic properties.[1] For example, flux and hydrothermal methods run solid state reactions at 150−500 °C for several hours or for days, and they are often classified as "intermediate temperature techniques".[2,3] In the case of some analogous methanothermal syntheses, the reaction temperature can be as low as 80 °C.[4]

Recently one of us developed a low-temperature method making use of ammonium salts of thiometallates for the synthesis of Mo(W)/Cu(Ag)/S clusters.[5] The heating temperatures are typically at ∼100 °C, and in some cases the reactions proceed even at room temperature, which is significantly lower than those in the intermediate-temperature flux method. A dozen Mo(W)/Cu(Ag)/S clusters prepared by this method were found to exhibit nonlinear optical (NLO) properties.[6−10] Then we communicated the successful introduction of thallium(I) ion and formation of the first W/Tl sulfide complex, $[(n\text{-Bu})_4N][TlWS_4]$.[11] However, the yields of the products obtained from the low-temperature method have been low, being in the 10% range or lower.

In an attempt to improve the yield of $[(n\text{-Bu})_4N][TlWS_4]$, we looked for other synthetic routes and found that microwave irradiation of a well-ground mixture of starting materials gave rise to the desired product in ∼1 min. The molybdenum analogue was also prepared in a similar manner. By controlling the microwave power and irradiation time, the yields can be raised to 25−26%. The microwave dielectric loss heating effects allow the reaction temperatures to go up to 500−1000 °C in very short periods of time, and thus greatly accelerate solid state reactions. This technique has been applied to preparations of various metal oxides,[12−14] metal chalcogenides,[15−17] and metal clusters of the groups 5 and 6 elements.[17] We herein report the facile microwave synthesis of $[(n\text{-Bu})_4N][TlMS_4]$ (**1**, M = Mo; **2**, M = W), their structures, and their NLO properties.

Experimental Section

Synthesis of $[(n\text{-Bu})_4N][TlMoS_4]$ (1). A well-ground mixture of $[NH_4]_2[MoS_4]$ (0.25 g, 1.0 mmol), TlBr (0.28 g, 1.0 mmol), and $[(n\text{-Bu})_4N]Br$ (0.96 g, 3.0 mmol) was placed in an open Pyrex glass tube which was stored in a large beaker in a domestic microwave oven equipped with a power control (National IEC-705: Hi (700 W); MedHi (500 W); Med (300 W); MedLo (100 W); Lo (50 W)). The irradiation power and time were set in the following order: MedHi, 15 s; MedLo, 10 s; Lo, 10 s; MedHi, 5 s; Lo, 10 s. After irradiation, the resulting dark red mixture was allowed to cool to room temperature and then extracted with DMF (3 mL) and filtered. Dark red needles of **1** formed from the filtrate on standing at ambient temperature for 1 day. Yield: 0.17 g (25.33%). Anal. Calcd for $C_{16}H_{36}MoNS_4Tl$: C, 28.64; H, 5.42; N, 2.09. Found: C, 28.35; H, 5.39; N, 2.17. UV−vis (CH_3CN) (λ_{max}/nm (ϵ/M^{-1} cm^{-1})): 459 (330), 353 (334), 308 (735), 267 (949), 244 (1233). IR (Nujol mull, CsI): 551 ν(Mo−S$_t$); 460 ν(Mo−S$_{br}$) cm^{-1}.

Synthesis of $[(n\text{-Bu})_4N][TlWS_4]$ (2). The tungsten analogue was obtained as yellow needles by a similar treatment of $[NH_4]_2[WS_4]$ (0.35 g, 1.0 mmol), where the microwave irradiation was controlled in the following order: MedHi, 20 s; Lo, 10 s; MedHi, 15 s; Lo, 10 s. Yield: 0.20 g (26.35%). Anal. Calcd for $C_{16}H_{36}NS_4TlW$ (**2**): C, 25.32; H, 4.79; N, 1.85. Found: C, 25.05; H, 4.75; N, 1.93. UV−vis (CH_3CN) (λ_{max},/nm (ϵ/M^{-1} cm^{-1})): 398 (775), 282 (1067), 221 (1697). IR (Nujol mull, CsI): 460 ν(W−S$_t$); 447 and 434 ν(W−S$_{br}$) cm^{-1}.

Physical Measurements. FT-IR spectra were recorded on a Jasco A-3 spectrophotometer. Samples for IR spectroscopy were typically mulls between CsI plates prepared using solid materials and Nujol. UV−vis spectra were measured on a Jasco V560 spectrophotometer. Carbon, hydrogen, and nitrogen analyses were carried out on a Perkin-Elmer 240C elemental analyzer.

The optical measurements was performed with linearly polarized 7-ns pulses at 532 nm generated from a frequency-doubled Q-switched Nd:YAG laser; the spacial profiles of the pulses were nearly Gaussian after a spacial filter was employed. The crystals of **1** and **2** are stable toward oxygen and moisture. The CH_3CN solution of 5.10×10^{-4} M for **1** or 4.90×10^{-4} M for **2** was placed in a 1-mm-thick quartz cell and the sample position was changed with respect to the focal plane ($z = 0$). The incident beam was focused into a spot radius (ω_0) of 35 mm (half-width at 1/e^2 maximum) by a 25-cm focal-length mirror. An aperture of 0.5-mm radius was placed in front of the transmission detector to assist the measurement of the refractive nonlinearity (referred to as a "closed aperture" *Z* scan, compared with an "open aperture" *Z* scan). The energies of the incident and transmission signals were measured by two Laser Precision detectors (RjP-735 and RjP-765 energy probes) which were linked to a computer by an IEEE interface. The interval of each transmittance measurement

---

[*] To whom correspondence should be addressed.
[†] Nagoya University.
[‡] Suzhou University.
[§] National University of Singapore.

(1) Stein, A.; Keller, S. W.; Mallouk, T. E. *Science* **1993**, *259*, 1558.
(2) Kanatzidis, M. G.; Park, Y. *J. Am. Chem. Soc.* **1989**, *111*, 3767.
(3) Dhingra, S.; Kanatzidis, M. G. *Science* **1992**, *258*, 1769.
(4) Das, B. K.; Kanatzidis, M. G. *Inorg. Chem.* **1995**, *34*, 1011.
(5) Lang, J. P.; Xin, X. Q. *J. Solid State Chem.* **1994**, *108*, 118.
(6) Shi, S.; Ji, W.; Tang, S. H.; Lang, J. P.; Xin, X. Q. *J. Am. Chem. Soc.* **1994**, *116*, 361.
(7) (a) Shi, S.; Ji, W.; Lang, J. P.; Xin, X. Q. *J. Phys. Chem.* **1994**, *98*, 3570. (b) Shi, S.; Ji, W.; Xin, X. Q. *J. Phys. Chem.* **1995**, *99*, 894. (c) Shi, S.; Hou, H. W.; Xin, X. Q. *J. Phys. Chem.* **1995**, *99*, 4050. (d) Chen, Z. R.; Hou, H. W.; Xin, X. Q.; Yu, K. B.; Shi, S. *J. Phys. Chem.* **1995**, *99*, 8717.
(8) Hou, H. W.; Xin, X. Q.; Liu, J.; Chen, M. Q.; Shi, S. *J. Chem. Soc., Dalton Trans.* **1994**, 3211.
(9) Shi, S.; Ji, W.; Xie, W.; Tang, S. H.; Zeng, H. C.; Lang, J. P.; Xin, X. Q. *Mater. Chem. Phys.* **1995**, *39*, 298.
(10) Sakane, G.; Shibahara, T.; Hou, H. W.; X. Q. Xin, X. Q.; Shi, S. *Inorg. Chem.* **1995**, *34*, 4785.
(11) Lang, J. P.; Liu, J.; Chen, M. Q.; Lu, J. M.; Bian, G. Q.; Xin, X. Q. *J. Chem. Soc., Chem. Commun.* **1994**, 2665.
(12) Baghurst, D. R.; Chippendale, A. M.; Mingos, D. M. P. *Nature*, **1988**, *332*, 311.
(13) Mingos, D. M. P.; Baghurst, D. R. *Chem. Soc. Rev.* **1991**, *20*, 1.
(14) Mingos, D. M. P.; Baghurst, D. R. *J. Chem. Soc., Chem. Commun.* **1988**, 829.
(15) Whittaker, A. G.; Mingos, D. P. M. *J. Chem. Soc., Dalton Trans.* **1992**, 2751.
(16) Landry, C. C.; Barron, A. R. *Science* **1993**, *260*, 1653.
(17) Whittaker, A. G.; Mingos, D. M. P. *J. Chem. Soc., Dalton Trans.* **1995**, 2073.

S0020-1669(96)01090-7 CCC: $12.00 © 1996 American Chemical Society

Table 1. Crystallographic Data for **1**

formula	$C_{16}H_{36}MoNS_4Tl$
fw	671.02
space group	*Cc* (No. 9)
crystal system	monoclinic
a (Å)	17.193(2)
b (Å)	18.354(1)
c (Å)	7.810(2)
β (deg)	97.19(1)
V (Å^3)	2445.2(5)
Z	4
ρ_{obsd}/ρ_{calcd} (g cm^{-3})	1.825/1.823
μ (Mo Kα) (cm^{-1})	74.25
radiation (λ (Å))	Mo Kα (0.710 69)
R	0.025[a]
R_w	0.028[b]

[a] $R = \sum||F_o| - |F_c||/\sum|F_o|$. [b] $R_w = [\sum w(|F_o| - |F_c|)^2/\sum w|F_o|^2]^{1/2}$.

Table 2. Postional Parameters for the Non-Hydrogen Atoms of **1**

atom	x	y	z	B_{eq}[a]
Tl	0.5448	0.07703(2)	0.9841	4.715(6)
Mo	0.53874(5)	−0.12725(3)	0.9854(1)	3.01(1)
S(1)	0.4575(1)	−0.0539(2)	0.8290(4)	4.30(5)
S(2)	0.6260(1)	−0.0598(1)	1.1424(3)	3.93(5)
S(3)	0.5949(1)	−0.1961(1)	0.8096(4)	4.34(5)
S(4)	0.4765(2)	−0.1909(2)	1.1583(4)	5.17(6)
N	0.3307(4)	0.2709(5)	0.103(1)	4.6(2)
C(1)	0.4077(5)	0.2935(6)	0.212(1)	5.6(2)
C(2)	0.4153(7)	0.3702(7)	0.283(2)	7.6(3)
C(3)	0.4998(9)	0.3828(8)	0.369(2)	11.4(5)
C(4)	0.5132(10)	0.454(1)	0.441(3)	12.2(6)
C(5)	0.3036(6)	0.3282(6)	−0.029(1)	5.7(2)
C(6)	0.3611(8)	0.3453(8)	−0.152(2)	8.7(4)
C(7)	0.324(2)	0.424(2)	−0.245(3)	20(1)
C(8)	0.276(2)	0.415(2)	−0.368(3)	15(1)
C(9)	0.2640(5)	0.2672(6)	0.216(1)	5.6(2)
C(10)	0.2726(8)	0.2147(8)	0.356(2)	7.3(4)
C(11)	0.1923(8)	0.2098(8)	0.436(2)	8.6(4)
C(12)	0.132(1)	0.1666(10)	0.350(3)	11.4(5)
C(13)	0.3458(6)	0.1981(5)	0.027(1)	5.4(2)
C(14)	0.2765(7)	0.1593(6)	−0.064(2)	7.1(3)
C(15)	0.3021(9)	0.0887(7)	−0.139(2)	7.8(4)
C(16)	0.237(1)	0.0422(10)	−0.219(3)	11.3(6)

[a] $B_{eq} = 8/3\pi^2(U_{11}(aa^*)^2 + U_{22}(bb^*)^2 + U_{33}(cc^*)^2 + 2U_{12}aa^*bb^* \cos\gamma + 2U_{13}aa^*cc^* \cos\beta + 2U_{33}bb^*cc^* \cos\alpha)$.

was set at 5 s so that every pulse of light was assured of meeting fresh molecules in the sample to eliminate the influence of any photon degradation.

X-ray Diffraction Crystallography. All measurements were made on a Rigaku AFC7R diffractometer at ambient temperature by using graphite-monochomatized Mo Kα radiation (0.710 69 Å). Crystallographic calculations were carried out with a teXsan crystallographic software package of the Molecular Structure Corp. (1985 and 1992). A dark red single crystal of **1** with dimensions 0.20 × 0.20 × 0.60 mm was mounted at the top of a glass fiber. Cell constants and an orientation matrix for data collection were obtained from least-squares refinements using the setting angles of 25 carefully centered reflections in the range $29.6° < 2\theta < 30.0°$. The intensities of three representative reflections monitored every 150 reflections showed no sign of crystal decay. An empirical absorption correction using the empirical ψ scan technique was applied, which resulted in transmission factors ranging from 0.84 to 1.00. The data were also corrected for Lorentz and polarization effects. Crystallographic data for **1** are summarized in Table 1. The structure was solved by heavy-atom Patterson methods and refined by difference Fourier methods.[18] The non-hydrogen atoms were refined anisotropically, and hydrogen atoms were included at calculated positions without refinement. The final R and R_w factors were 0.025 and 0.028, respectively, for 2294 unique reflections with $I > 3.00\sigma(I)$. The maximum and minimum peaks on the final difference Fourier map correspond to 0.36 and −0.77 e/Å^3. We have considered the centrosymmetric space group *C2/c*. With this space group, Mo and Tl sit on a twofold axis, so that S1 and S2 become equivalent as are S3 and S4. These atoms were located properly. Although another twofold axis is expected to run through the N atom of the cation, we found that the N site is disordered at two (or more) general positions. From the subsequent Fourier synthesis, carbon atoms of the cation could not be located well, and the R value did not go down below 8%. Therefore, the space group of *C2/c* was ruled out. Atomic coordinates and equivalent isotropic thermal parameters are given in Table 2.

Results and Discussion

Microwave Irradiation Synthesis. During the microwave irradiation, an argon stream was introduced into the reaction tube for safe removal of the NH_3 and H_2S gases evolved. When the high-power irradiation (Hi) was applied, both the molybdenum and tungsten reaction mixtures melted immediately and began to bubble violently within 20 s. Extraction of the resulting solid with DMF gave a nearly colorless filtrate, from which we were unable to isolate **1** or **2**. Under this heating condition, $[NH_4]_2[MS_4]$ appeared to decompose into less soluble WS_3 and clusters with high nuclearity, e.g., $[W_3S_9]^{2-}$.[19] Application of the MedHi power level again resulted in melting of the reaction mixtures in a short irradiation time. However, the molten state could be maintained as the power level was quickly lowered to Med and Lo after 10−20-s irradiation at the MedHi level. In this case, bubbling of the samples did not take place. Thus, careful control of the microwave power and irradiation time is critically important for the solid state synthesis of **1** and **2**. Although it is not possible to estimate the actual magnitude of the absorption of the microwaves by the sample, which will become necessary to optimize the reaction condition in a rational way, 25−26% yields of **1** and **2** attained by "visual control" are acceptable at moment, being 3 times higher than those in our previous low-temperature method. On the other hand, in the standard solution reaction of $[NH_4]_2[MS_4]$, TlBr, and $[(n\text{-Bu})_4N]Br$ in DMF at 100 °C for 12 h, formation of **1** and **2** were not discernible.

Crystal Structure. According to X-ray analysis, **1** has the one-dimensional structure as shown in Figure 1. The $[TlMoS_4]_n^{n-}$ chains are separated by $[(n\text{-Bu})_4N]^+$ ions, and no hydrogen bond interaction exists between the chain and the *n*-Bu hydrogens. The chains are composed of MoS_4 tetrahedra connected by Tl atoms as illustrated in Figure 2. The repeating unit within the chain is $TlMoS_4$, where Mo, S1, S2, and Tl are nearly coplanar, as are Mo, S3, S4, and Tl. This unit is stacked along the crystallographic *c* axis with the Mo → Tl vectors pointing alternatively right and left. Looking down the *c* axis, one may view the chain as a three-layered tape in which the Tl−Mo layer is sandwiched by two sulfur layers consisting of S2−S3 and S1−S4. There are four crystallographically independent sulfur atoms, and they are grouped into two classes: triply-bridging sulfurs, S1 and S2, and doubly-bridging sulfurs, S3 and S4. The Mo−S bond lengths of 2.167(3)−2.198(3) Å are normal, while the Tl−S bond distances are variegated and range from 3.007(3) to 3.387(3) Å. The average Tl−S distance of 3.214 Å falls in between the $Tl^{2+}-S^{2-}$ length of 2.70 Å and $Tl^{+}-S^{2-}$ length of 3.34 Å estimated from each ionic radius.[20] The long Mo−Tl distance (3.7509(7) Å) indicates that their bonding interactions, if any, should be very weak.

---

(18) Beurskens, P. T.; Admiraal, G.; Beurskens, G.; Bosman, W. P.; Garcia-Granda, S.; Gould, R. O.; Smits, J. M. M. and Smykalla, C. The DIRDIF Program System, Technical Report of the Crystallography Laboratory, University of Nijmegen, Nijmegen, The Netherlands, 1992.

(19) Koniger-Ahlborn, E.; Müller, A. *Angew. Chem., Int. Ed. Engl.* **1975**, *14*, 574.

(20) Shannon, R. D. *Acta Crystallogr.* **1976**, *A32*, 751.

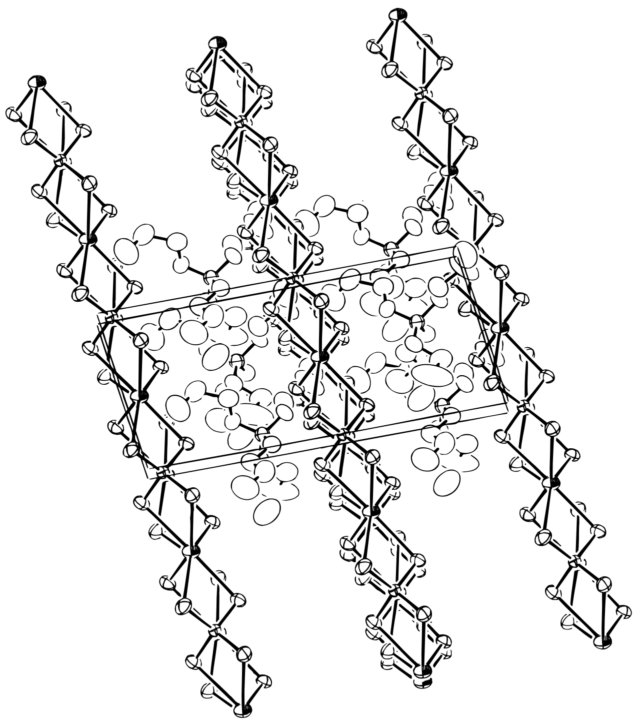

Figure 1. Extended structure of [(*n*-Bu)$_4$N][TlMoS$_4$] (**1**) looking down the *b* axis.

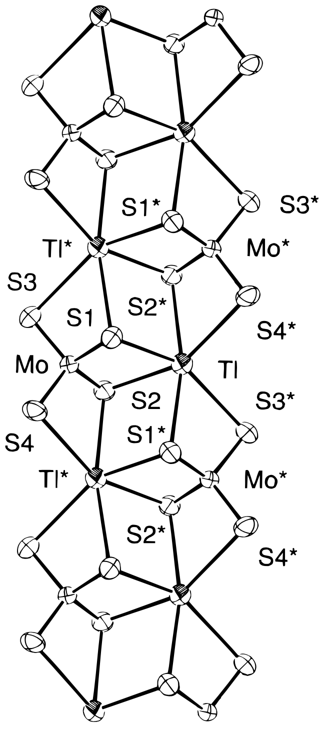

Figure 2. ORTEP drawing of one polymeric chain in [(*n*-Bu)$_4$N]-[TlMoS$_4$] (**1**) (parallel to the crystallographic *c* axis). Thermal ellipsoids are depicted at the 50% probability level. Selected bond lengths (Å) and angles (deg): Tl−Mo 3.7509, Tl−S1 3.271(3), Tl−S2 3.180(3), Tl−S3 3.381(3), Tl−S4 3.387(7), Tl−S1* 3.007(3), Tl−S2* 3.058-(3), Mo−S1 2.197(3), Mo−S2 2.198(3), Mo−S3 2.178(3), Mo−S4 2.167(3) Å; S1−Tl−S3* 152.49(7), S2−Tl−S4* 155.23(7), S1*−Tl−S2* 166.76(5), Mo−Tl−S1 81.51(5), Mo−Tl−S2 85.28(5), S1−Mo−S2 107.88(7), S1−Mo−S3 107.8(1), S1−Mo−S4 110.4(1), and S3−Mo−S4 111.88(9)°.

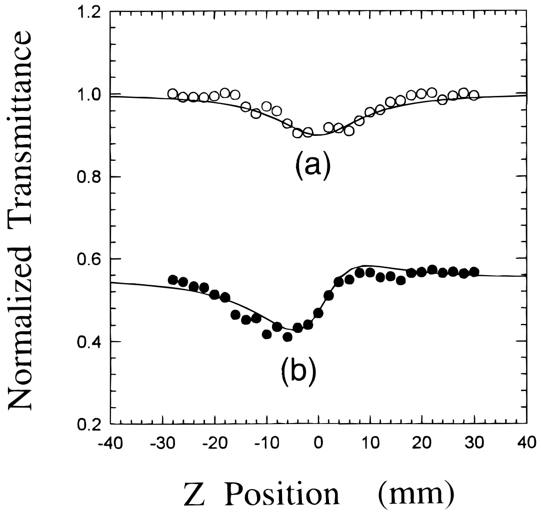

Figure 3. *Z*-scan data of 5.10 × 10^{-4} M **1** at 532 nm with $I_0 = 1.70 \times 10^{-9}$ W/m^2. (a) The data shown by open circles are those collected under an open aperture configuration, and the solid curve is a theoretical fit based on

$$T(Z) = (1/(\pi)^{1/2}q(Z))\int_{-\infty}^{\infty}\ln[1+q(Z)]e^{-\tau^2}\,d\tau \text{ and } q(Z) = \alpha_2 I(Z)(1-e^{-\alpha_0 L})/\alpha_0.$$

(b) The data shown by filled circles were obtained by dividing the normalized *Z*-scan data measured under closed aperture configuration by the normalized *Z*-scan data of (a).

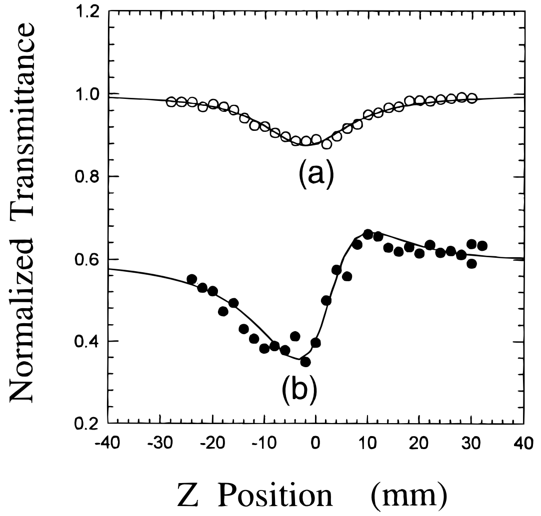

Figure 4. *Z*-Scan data of 4.90 × 10^{-4} M of **2** at 532 nm with $I_0 = 3.48 \times 10^{-9}$ W/m^2. (a) The data shown by open circles are those collected under an open aperture configuration, and the solid curve is a theoretical fit based on

$$T(Z) = (1/(\pi)^{1/2}q(Z))\int_{-\infty}^{\infty}\ln[1+q(Z)]e^{-\tau^2}\,d\tau \text{ and } q(Z) = \alpha_2 I(Z)(1-e^{-\alpha_0 L})/\alpha_0.$$

(b) The data shown by filled circles were obtained by dividing the normalized *Z*-scan data measured under closed aperture configuration by the normalized *Z*-scan data of (a).

Nonlinear Optical Properties. The nonlinear optical properties of **1** and **2** were investigated in acetonitrile using a *Z*-scan technique.[21] The "open" and "closed" *Z*-scan data are given in Figures 3 and 4. The observed curves clearly show the presence of both nonlinear optical absorption and nonlinear optical refraction. The valley−peak pattern of the normalized transmittance curve obtained under a close aperture configuration shows characteristic self-focusing behavior of propagating light in the sample.

---

[21] Riddick, J. A.; Bunger, W. B.; Sakano, T. K. *Organic Solvents: Physical Properties and Method of Purification*, 4th ed.; John Wiley and Sons: New York, 1986.

The nonlinear absorption component was evaluated under an open aperture configuration. Theoretical curves of transmittance against the Z position were fitted to the observed Z-scan data by varying the α_2 value, where the experimentally measured α_0, L, and $I_i(z)$ values were adopted. The solid curves in Figures 3a and 4a are the theoretical curves calculated with $\alpha_2 = 2.2 \times 10^{-7}$ m/W for **1** and $\alpha_2 = 1.8 \times 10^{-7}$ m/W for **2**. The nonlinear refractive components of **1** and **2** were assessed by dividing the normalized Z-scan data obtained under the closed aperture configuration by those obtained under the open aperture configuration. They are plotted in Figures 3b and 4b, and the theoretical curves are superimposed for comparison where the n_2 values estimated therefore are 3.1×10^{-14} m^2/W for **1** and 3.2×10^{-14} m^2/W for **2**, respectively. The acetonitrile solutions of **1** and **2** cause self-focusing of the propagating light, while acetonitrile itself is known to show a negative dn/dT of -4.5×10^{-4} K^{-1} .[20] Therefore, the observed NLO properties are not due to the solvent thermal effect.

Although the concentrations of **1** and **2** in solution are currently limited because of their poor solubility, larger n_2 value for both **1** and **2** would be expected if higher concentrations are attained, and if formation of a thin film is engineered. The successful synthesis of **1** and **2** by a microwave irradiation method illustrates the potential applicability of the method to the quick and facile preparation of novel Mo(W)/S compounds with NLO properties.

Acknowledgment. J.P.L. acknowledges support of a post-doctoral fellowship by the Japanese Society for the Promotion of Science.

Supporting Information Available: Tables giving crystallographic data, bond lengths, bond angles, torsion angles, anisotropic displacement parameters for the non-hydrogen atoms and atomic coordinates for hydrogen atoms, least-square planes, and cell packing diagram of **1** and text describing the experimental details of nonlinear optical properties of **1** and **2** (31 pages). Ordering information is given on any current masthead page.

IC9610905